Supplementary information

Organic carbon speciation

The results of the organic carbon speciation are reported in Table S1.

Table S1: TC400-ROC-TOC analyses on carbonate rocks. Values are the average of two different determinations. Symbols legend: TC400 = total carbon at 400 °C, ROC = residues oxidizable carbon at temperatures between 400 and 600 °C; TOC = total organic carbon; Dev.St = standard deviation of TOC values.

No.	Sample	TOC400	ROC	TOC	Dev.St
		Wt%	Wt%	Wt%	Wt%
1	HOS-1	0.0485	0.0520	0.1010	0.017
2	HOS-2	0.0365	0.1290	0.1655	0.002
3	HOS-3	0.0450	0.0635	0.1080	0.031
4	HOS-4	0.0345	0.0935	0.1280	0.011
5	HOS-5	0.0615	0.1520	0.2135	0.008
6	QSC-1	0.0475	0.0610	0.1085	0.023
7	USI-1	0.0460	0.0625	0.1085	0.040
8	USI-2	0.0490	0.0805	0.1295	0.018
9	USI-3	0.1090	0.0500	0.1590	0.095
10	USI-4	0.0600	0.0655	0.1255	0.002
11	USI-5	0.0680	0.0405	0.1085	0.052
12	USI-6	0.0515	0.0775	0.1285	0.067
13	USI-7	0.0680	0.0625	0.1310	0.045
14	USI-8	0.0295	0.0725	0.1020	0.041
15	USI-9	0.0885	0.1095	0.1990	0.018
16	QSC-2	0.0565	0.1000	0.1565	0.035
17	USI-10	0.0405	0.1460	0.1865	0.036
18	USI-11	0.0785	0.1785	0.2570	0.014
19	USI-12	0.0710	0.2625	0.3335	0.053
20	USI-13	0.0420	0.1940	0.2360	0.016
21	USI-14	0.0450	0.1645	0.2100	0.031
22	USI-15	0.0765	0.1950	0.2715	0.042
23	USI-16	0.0535	0.2455	0.2990	0.001

The total organic carbon of the investigated rocks varies from 0.101 to 0.335 wt%, a range compatible with that found in commercial limestones (0.01-0.5 wt%) [1]. Dolostones and limestone show distinct organic carbon contents and speciation. In particular, dolostones generally show a higher total organic carbon (TOC = TOC400 + ROC) than limestones with values ranging between 0.187 and 0.335 wt% and between 0.101 and 0.214 wt%, respectively, with the exception of the dolostone sample QSC-2 displaying a relatively low TOC value (0.157 wt%). The higher TOC range showed by dolostone results from their higher residual oxidizable carbon (ROC) contents (0.146-0.263 wt%) with respect to limestones (0.041-0.152 wt%), except for sample QSC-2 that shows a ROC value of 0.1 wt%. The thermally labile organic carbon TOC400 contents of dolostone and limestones are instead overlapping, with the former ranging between 0.057 and 0.079 wt% and the latter between 0.0295 and 0.089 wt%, respectively. The ROC contribution to the TOC is generally higher in dolostones (median value of 78%) than in limestones (median value of 58%). On the whole, the organic carbon content of the investigated rocks doesn't show any significant correlation with the other analytical results.

EPR fingerprints

The results of the EPR spectroscopic investigation of the samples, reported in Table S2, revealed a number of interesting features (see Fig. S1). The resulting 23 spectra can be grouped according to four main spectral features, as detailed below. All spectral features due to Mn(II) ions have been parameterized according to a standard procedure found in the literature [2]; the reader is referred to this article for further information on this procedure (Table S2).

Table S2: Results of the EPR spectral parameterisation. Values are referred to three different species in the spectra: Mn in 1) the calcic site in calcite (cc), 2) the magnesian site in dolomite (dol) 3) a pseudoisotropic site (3rd). The spread parameter was determined in all the species, whereas the spli and wav parameters were determined only in the prevailing species (cc or dol). The last column reports the categorical (presence/absence) information about the organic radical species. Symbol legend: = present.

Sample	Spread cc	Spread dol	Spread 3rd	Spli cc	Spli dol	Wav cc	Wav dol	dolom	% Mn Ca_cc	% Mn Mg_dol	% Mn 3rd	radical
HOS1	486.97			14.07		3.44		0.00	100.00	0.00	0.00	
HOS2	487.36			13.98		3.82		0.00	100.00	0.00	0.00	
HOS3	487.08			13.91		3.73		0.00	100.00	0.00	0.00	
HOS4	487.17			13.88		3.94		0.00	100.00	0.00	0.00	
HOS5	487.43			13.79		4.23		0.00	100.00	0.00	0.00	
QSC1	487.54			13.85		4.28		0.00	100.00	0.00	0.00	
USI1	487.37			14.05		3.58		0.00	100.00	0.00	0.00	
USI2	487.02			14.09		3.61		0.00	100.00	0.00	0.00	
USI3	487.37			14.09		3.78		0.00	100.00	0.00	0.00	
USI4	486.96			13.80		3.82		0.00	100.00	0.00	0.00	
USI5	487.29			13.62		4.17		0.00	100.00	0.00	0.00	
USI6	487.49			13.83		4.22		0.00	100.00	0.00	0.00	
USI7	487.17			13.69		4.55		0.00	100.00	0.00	0.00	
USI8	490.79	519.82		13.67		4.40		0.51	66.02	33.98	0.00	
USI9	487.25			13.95		3.72		0.00	100.00	0.00	0.00	
QSC-2		520.68	474.64		49.69		8.76	2.05	0.00	67.24	32.76	
USI10		520.26	473.72		50.23		7.72	3.03	0.00	75.21	24.79	
USI11		519.51	474.11		49.88		8.24	2.01	0.00	66.79	33.21	
USI12		519.69	474.07		49.77		7.59	3.34	0.00	76.98	23.02	
USI13		519.64	474.18		49.78		7.66	0.87	0.00	46.43	53.57	
USI14		519.84	474.38		50.32		7.31	1.00	0.00	50.09	49.91	
USI15	487.45	519.84			49.90		7.63	1.09	47.89	52.11	0.00	
USI16		519.31	473.88		49.36		7.71	1.90	0.00	65.52	34.48	

Figure S1. Representative EPR spectra, registered at X-band and room temperature, highlighting all features described in the text: a) typical pattern of Mn(II) in the Ca site in calcite; b) spectrum arising from the superposition of a spectrum closely resembling that in a) and another due to Mn(II) in the Mg site in dolomite; c) spectrum arising from the superposition of the features due to Mn(II) in the Mg site in dolomite and those arising from Mn(II) in a third crystal chemical configuration; d) spectrum of "calcitic" Mn(II) exhibiting, highlighted by the dashed ellipse, the signal due to the organic radical species.

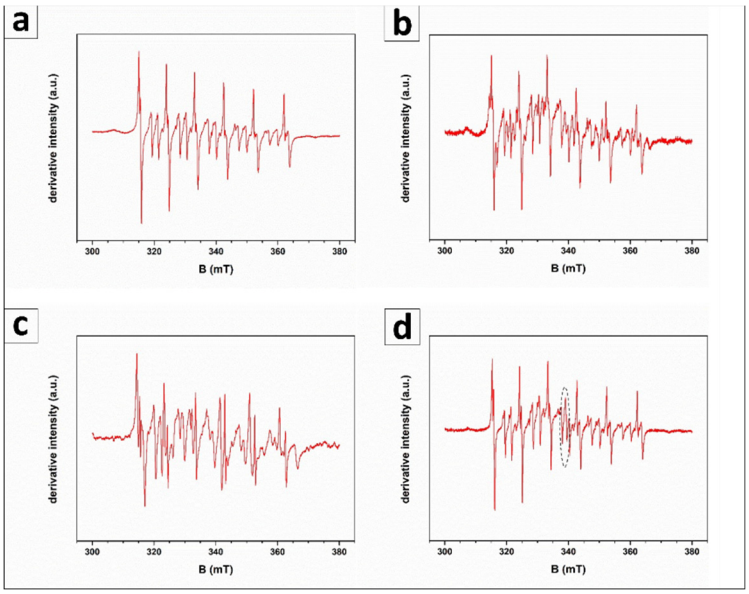

14 spectra (Fig. S1a) show the typical features ascribed in the literature to the presence of diluted Mn(II) ions in the Ca site of calcite [2] [3] [4] [5]. Basically, the replacement of Ca by Mn in a distorted octahedral site gives rise to a series of interactions (hyperfine interaction between unpaired electrons and the magnetic Mn nucleus, fine interaction between the five unpaired electrons of Mn(II), a distribution of the fine interaction due to subordinate effects resulting from the local speciation in the second shell of the paramagnetic center) that well explain the spectral complexity. This spectral type is hereafter referred to as "calcitic Mn".

2 spectra (Fig. S1b) show the features already described for the previous group and, superimposed, additional features that can be attributed [6] to the presence of Mn(II) ions in the Mg site of dolomite. This double carbonate can, in fact, host the replacement of divalent cations by Mn in the two crystallographically inequivalent Mg and Ca sites. In particular, the Mg site has a lower volume [7]. This condition induces an enhancement of the hyperfine and fine interactions, then a more pronounced splitting of the resulting spectrum. This subspectrum will be referred to as "dolomitic Mn (Mg site)".

7 spectra (Fig. S1c) still appear to be contributed by two superimposed subspectra: the first one is the dolomitic Mn (Mg site), but the second is not the calcitic Mn. On the other hand, a well-defined sextet is observed, showing almost no fine interaction and consequently no distribution of the fine interaction. We speculate on the possible assignment of this further subspectrum. In particular, considering the strength of the hyperfine interaction, almost coincident with that of the

"calcitic Mn", we attribute the subspectrum to Mn(II) ions replacing Ca in the Ca sites in dolomite. Since these sites are larger than the Ca sites in calcite [7] a resulting decrease in the fine interaction could be justified. This subspectrum is hereafter referred to as "dolomitic Mn (Ca site)".

Another group, consisting of 8 samples, can be transversally defined according to a fourth relevant feature: the appearance of an extra single signal (Fig. S1d), occurring at a magnetic field value that allows a direct attribution to radical(s) originating from organic matter finely dispersed in the samples. 7 samples of the 1st group, and one of the 2nd group show this feature (Table S2).

Thus, according to the EPR results, Mn seems to be either distributed only in calcite (regardless of the chemical and mineralogical composition of the samples) or distributed between calcite and dolomite (but in a way in principle independent of the calcite/dolomite ratio in the samples), or finally distributed between two metal sites in dolomite, allowing the estimation of a distribution coefficient internal to this mineral.

Supplementary information from the plant

Quicklime and dololime production campaigns at USI plant during the year 2021 is reported in. Table S3.

Table S3: The fundamental compositional and technical parameters of burnt lime products, including calcium oxide, magnesium oxide, slaking reactivity (referred as t_{50} or t_{60}) and residual CO_2 content.

Feeding material	Final product	Period	CaO	MgO	t_{50}-t_{60}	CO_2
			[wt%]	**[wt%]**	**[min]**	**[wt%]**
USI-12	Dololime	01-10 Jan 2021	60.2	25.6	3.9	7.8
USI-5	Quicklime	11-16 Jan 2021	88.8	6.1	2.2	4.4
USI-12	Dololime	17-27 Jan 2021	62.6	29.2	3.7	7.3
USI-5	Quicklime	28-Jan - 4-Feb 2021	90.5	2.3	2.1	6.4
USI-12	Dololime	4-Feb -31-Mr 2021	63.0	30.6	4.2	5.3
USI-5	Quicklime	1-12 Apr 2021	89.4	6.2	3.4	3.6
USI-12	Dololime	13-20 Apr 2021	62.3	31.9	3.6	4.2
USI-15	Dololime	21-Apr 8-Maj 2021	59.7	32.4	0.5	3.4
USI-5	Quicklime	9-28-Maj 2021	89.8	2.7	4.0	5.0
USI-12	Dololime	28-Maj 4-Jun 2021	61.4	31.3	3.0	4.1
USI-15	Dololime	5-Jun 29-Jul 2021	60.5	32.8	0.5	3.6
USI-5	Quicklime	29-Jul-21	88.0	2.4	3.6	7.2
USI-8	Quicklime	30-Jul 4-Aug 2021	91.6	1.5	1.8	4.7
USI-15	Dololime	5-28 Aug 2021	62.3	30.6	0.7	4.5
USI-8	Quicklime	29-Aug 12-Oct 2021	79.9	1.9	1.3	4.7
USI-15	Dololime	13-Oct 3-Nov 2021	62.9	31.9	0.4	2.4
USI-8	Quicklime	4-14 Nov 2021	92.0	3.5	1.0	2.6
USI-15	Dololime	15-26 Nov 2021	61.5	32.7	0.4	3.1
USI-8	Quicklime	27-Nov 8-Dec 2021	88.6	5.7	1.0	3.4
USI-15	Dololime	8-Dic 28-Dec 2021	61.6	32.5	0.5	3.1
USI-8	Quicklime	28-31 Dec 2021	92.0	2.2	0.9	2.8

References

[1] J. Oates, *Lime and Limestone. Chemistry and technology, production and uses;* Wiley-VCH: Weinheim, 1998, p. 177.

[2] D. Attanasio, M. Brilli e N. Ogle, *The Isotopic Signature of Classical Marbles;* L'Erma di Bretschneider: Roma, 2006, p. 297.

[3] M. Romanelli, A. Buccianti, F. Di Benedetto, L. Bellucci e S. Cemicky, An innovative electron paramagnetic resonance and statistical analysis approach to investigate the geographical origin of multi-layered samples from a Renaissance painting. *Microchemical Journal,* **2022**, *177*, 107219.

[4] S. Piligkos, I. Laursen, A. Morgenstjerne e H. Weihe, Sign and magnitude of Spin Hamiltonian parameters for Mn2+ impurities in calcite. A multi- and low-frequency EPR study. *Mol. Phys.,* **2007**, *115*, 2025–2050.

[5] A. Vassilikou-Dova, EPR-determined site distributions of low concentrations of transition-metal ions in minerals: review and predictions. *Am. Miner.*,**1993**, *78*, 1-2, 49-55.

[6] R. Shepherd e W. Graham, EPR of Mn2+ in polycrystalline dolomite. *J. Chem. Phys.,* **1984**, 81, 6080–6084.

[7] R. Reeder e S. Markgraf, High-temperature crystal chemistry of dolomite. *American Mineralogist,* **1986**, *71*, 5-6, 795-804.